EVALUATION OF TAMARIND (*TAMARINDUS INDICA L*) SHELL TANNIN EXTRACTS AS A CORROSION INHIBITOR OF MILD STEEL IN ACIDIC MEDIUM

ABDULLAHI ABDULMAJID

UNIVERSITI SAINS MALAYSIA

2020

EVALUATION OF TAMARIND (*TAMARINDUS INDICA L*) SHELL TANNIN EXTRACTS AS A CORROSION INHIBITOR OF MILD STEEL IN ACIDIC MEDIUM

by

ABDULLAHI ABDULMAJID

Thesis submitted in fulfillment of the requirement
for the degree of
Doctor of Philosophy

June 2020

ACKNOWLEDGEMENT

All praises go to Allah the merciful the magnificent for the successful completion of this work, then my deep gratitude to my supervisor, Dr. Mohd Hazwan Hussin for his kindness, generosity and meticulous care. His insightful ideas and fruitful observations have been a key formative guidance on the present work. He has helped me in many possible ways since the commencement of my research. I also extend my sincere gratitude to my co-supervisor; Prof. Afidah Abdul Rahim for her careful and critical reading of my writing, without their encouragement and guidance, this research would have never derived out in the present form. Also, it has been enjoyable experience and memorable for me to work with them.

I would like also to thank Tertiary Education Trust fund (Tetfund) for providing me scholarship and Universiti Sains Malaysia for the research Grant Scheme 304/PKIMIA/6315100 to support this work.

Special thanks are due to all administrative and technical staff members of School of Chemical Sciences and Archeology Research Centre for their endless support. My appreciation also goes to Mr, Ali for his help in experimental work.

I would also extend my sincere appreciation to my lab mates, especially Tuan Hamidon, Adilla Binti Rozuli, Hanis Latif, Shahadad, Saraya, Fatin, Nabila, Mira and Liza for their helped and create a friendly environment during my study.

Furthermore, I would also like to extend my sincere gratitude to my father Mr. Bature Abdullahi, my mother Ms, Rabi Abdullahi, my grandfather Mr, Umar Abdullahi (Walin Hausa), my aunty Ms, Rabi Umar Sodangi my wife and children and my siblings for their support and encouragement. May Allah bless you all.

TABLE OF CONTENTS

ACKNOWLEDGEMENT ..... **ii**

TABLE OF CONTENTS ..... **iii**

LIST OF TABLES ..... **viii**

LIST OF FIGURES ..... **xi**

LIST OF ABBREVIATIONS ..... **xvi**

LIST OF SYMBOLS ..... **xviii**

ABSTRAK ..... **xx**

ABSTRACT ..... **xxii**

CHAPTER 1 INTRODUCTION **1**

1.1 Background of the study 1

1.2 Problem statement 4

1.3 Research objectives 5

1.4 Scope of the research 6

1.5 Limitation of the research 7

CHAPTER 2 LITERATURE REVIEW **8**

2.1 Tamarind 8

2.2 Tannins 10

2.3 Brief overview of corrosion 13

2.4 Corrosion of steel 16

2.5 Consequences of corrosion 20

2.6 Economic implications of corrosion 20

2.7 Corrosion control 21

2.7.1 Material selection 21

2.7.2 Proper design 22

2.7.3 Galvanic method 24

2.7.4 Impressed current systems 25
2.7.5 Corrosion inhibitors 26
2.7.6 Inorganic inhibitors 27
2.7.7 Organic inhibitors 29
2.7.8 Sol-gel and coating applications 31
2.7.9 Rust converters 37
2.8 Extraction methods of tannins 39
2.9 Corrosion measurement techniques 41
2.9.1 Electrochemical impedance spectroscopy (EIS) 41
2.9.2 Potentiodynamic polarization measurement (PD) 46
2.9.3 Electrochemical noise (EN) 50
2.10 Adsorption process in inhibition 52
2.10.1 Adsorption isotherm 54
CHAPTER 3 EXPERIMENTAL 57
3.1 Preparation of tamarind shell (TS) 57
3.2 Extraction of tamarind shell tannins 57
3.3 Physicochemical characterization of Tamarind shell extract 59
3.3.1 Fourier transform infrared (FTIR) spectroscopy 59
3.3.2 Nuclear magnetic resonance (NMR) spectroscopy 59
3.3.3 Thermal gravimetric analysis (TGA) 59
3.4 Phytochemical assays of tamarind shell extract 60
3.4.1 Total phenolic content (TPC) 60
3.4.2 Total flavonoid content (TFC) 60
3.4.3 Total tannin content (TTC) 61
3.4.4 Reducing power antioxidant assay 62
3.5 Rust Conversion Studies 62
3.5.1 Preparation of rust powder 62

3.5.2 FTIR analysis of rust 63
3.5.3 Effect of concentration 63
3.5.4 Effect of pH 64
3.5.5 Effect of reaction time 64
3.5.6 X-Ray diffraction analysis (XRD) 64
3.6 Corrosion inhibition studies 65
3.6.1 Preparation of mild steel plates 65
3.6.2 Preparation of electrolyte 65
3.6.3 Electrochemical cell and electrodes 65
3.6.4 Electrochemical impedance spectroscopy (EIS) 66
3.6.5 Potentiodynamic polarisation (PD) 66
3.6.6 Electrochemical noise (EN) 67
3.6.7 Effect of temperature 68
3.6.8 Adsorption isotherm studies 68
3.6.9 Surface analysis 68
3.7 Corrosion studies on TSTE extracts doped hybrid sol-gel 69
3.7.1 Preparation of hybrid sol-gel film 69
3.7.2 Electrochemical impedance spectroscopy (EIS) 70
3.7.3 Potentiodynamic polarisation (PD) 70
3.7.4 FT-IR study 70
3.7.5 Water contact angle measurement 71
3.7.6 Surface morphology analysis 71
CHAPTER 4 RESULTS AND DISCUSSION 72
4.1 Tamarind shell tannin extracts (TSTE) 72
4.2 Characterization of tamarind shell tannin extracts (TSTE) 73
4.2.1 Fourier transforms infrared spectroscopy (FTIR) 73
4.2.2 Nuclear magnetic resonance (NMR) 77

4.3 Phytochemical analysis of Tamarind shell (TSTE) extracts 80
4.3.1 Total phenolic content (TPC) 80
4.3.2 Total flavonoid content (TFC) 82
4.3.3 Total tannin content (TTC) 83
4.3.4 Reducing power assay 84
4.4 Thermal analysis (TGA) 86
4.5 Rust conversion studies 89
4.5.1 FTIR analysis of rust 89
4.5.2 The effect of concentration 90
4.5.3 The effect of pH 94
4.5.4 Effect of reaction time 96
4.5.5 FTIR signals of ferric tannate 98
4.5.6 Mechanism of rust transformation 99
4.5.7 XRD analysis 100
4.5.8 SEM analysis 102
4.6 Corrosion inhibition study 105
4.6.1 Electrochemical impedance spectroscopy (EIS) 105
4.6.2 Potentiodynamic polarization (PD) 114
4.6.3 Electrochemical noise measurement (ENM) 123
4.6.4 Effect of temperature 126
4.6.5 Adsorption isotherm process 132
4.6.6 Mechanism of corrosion inhibition 139
4.6.7 Surface analysis 141
4.7 Corrosion inhibition studies of hybrid sol-gel coatings 145
4.7.1 Electrochemical impedance spectroscopy (EIS) 145
4.7.2 Potentiodynamic polarization (PD) 157
4.7.3 Effect of temperature 165

4.7.4 FTIR study 168

4.7.5 SEM/EDX analysis 171

4.7.6 Water contact angle measurement 175

CHAPTER 5 CONCLUSION AND FUTURE RECOMMENDATIONS 177

5.1 Conclusion 177

5.2 Future recommendations 180

REFERENCES 181

APPENDICES

LIST OF PUBLICATIONS, CONFERENCES AND EXHIBITIONS

LIST OF TABLES

Page

Table 2.1	Studies on different types of natural plants as organic corrosion inhibitors	30
Table 2.2	Studies on corrosion protection of doped sol-gel coatings on steel substrates	36
Table 2.3	Summarizes the literature review towards the objective of the thesis.	56
Table 4.1	The extraction yield of TS using different solvents at room temperature	72
Table 4.2	The infrared absorption bands of all TSTE (TME, TAE, TWE, and TEAE)	76
Table 4.3(a)	^{13}C NMR peak assignment of all TSTE (TME, TAE, TWE and TEAE)	79
Table 4.3(b)	^{1}H- NMR chemical shift assignment of TAE, TEAE, TME and TWE	80
Table 4.4	Total phenolic content of TS extracts with different types of solvents	82
Table 4.5	Total flavonoid content of TS extracts with different types of solvents	83
Table 4.6	Total tannin content of TS extracts with different types of solvents	84
Table 4.7	The Nyquist impedance parameters at different concentrations of TME at 303 K	113
Table 4.8	The Nyquist impedance parameters at different concentrations of TAE at 303 K	113
Table 4.9	The Nyquist impedance parameters at different concentrations of TWE at 303 K	114
Table 4.10	The Nyquist impedance parameters at different concentrations of TEAE at 303 K	114
Table 4.11	Electrochemical polarization parameters for mild steel in 0.5M HCl solution in the absence and presence of TME at 303 K.	118

Table 4.12 Electrochemical polarization parameters for mild steel in 0.5M HCl solution in the absence and presence of TAE at 303 K..... 119

Table 4.13 Electrochemical polarization parameters for mild steel in 0.5M HCl solution in the absence and presence of TWE at 303 K..... 120

Table 4.14 Electrochemical polarization parameters for mild steel in 0.5M HCl solution in the absence and presence of TEAE at 303 K..... 121

Table 4.15 The noise resistance parameters for 1000 ppm of TS extracts at 303 K 125

Table 4.16 The thermodynamic parameters of mild steel dissolution in 0.5 M HCl solution to varying concentrations of TME at (303-333 K)..... 130

Table 4.17 The thermodynamic parameters of mild steel dissolution in 0.5 M HCl solution at different concentrations of TAE at (303-333 K)..... 130

Table 4.18 The thermodynamic parameters of mild steel dissolution in 0.5 M HCl solution at different concentrations of TWE at (303-333 K)..... 131

Table 4.19 The thermodynamic parameters of mild steel dissolution in 0.5 M HCl solution at different concentrations of TEAE (303-333 K) 131

Table 4.20 The adsorption parameters upon potentiodynamic polarization measurement at different concentrations of TME at 303 K 136

Table 4.21 The adsorption parameters upon potentiodynamic polarization measurement at different concentrations of TAE at 303 K..... 136

Table 4.22 The adsorption parameters upon potentiodynamic polarization measurement at different concentrations of TWE at 303 K..... 137

Table 4.23 The adsorption parameters upon potentiodynamic polarization measurement at different concentrations of TEAE at 303 K 137

Table 4.24 The EDX analysis of the percentage atomic content of mild steel in 0.5 M HCl 143

Table 4.25 Nyquist impedance parameters at various concentrations of TME Hybrid doped sol-gel at 303 K. 153

Table 4.26 Nyquist impedance parameters at various concentrations of TAE doped Hybrid sol-gel at 303 K..... 154

Table 4.27 Nyquist impedance parameters at various concentrations of TWE doped Hybrid sol-gel at 303 K..... 155

Table 4.28 Nyquist impedance parameters at various concentrations of TEAE doped Hybrid sol-gel at 303 K. 156

Table 4.29 Tafel parameters of undoped and TME doped hybrid sol-gel and their comparison with the bare mild steel in 0.5 M HCl solution at 303 K..... 161

Table 4.30 Tafel parameters of undoped and TAE doped hybrid sol-gel and their comparison with the bare mild steel in 0.5 M HCl solution at 303 K..... 162

Table 4.31 Tafel parameters of undoped and TWE doped hybrid sol-gel and their comparison with the bare mild steel in 0.5 M HCl solution at 303 K..... 163

Table 4.32 Tafel parameters of undoped and TEAE doped hybrid sol-gel and their comparison with the bare mild steel in 0.5 M HCl solution at 303 K..... 164

Table 4.33 The thermodynamic parameters of bare and hybrid sol-gel doped mild steel in 0.5 M HCl solution at (303 – 333 K)..... 167

Table 4.34 FT-IR spectra of hybrid sol-gel matrix, hybrid sol-gel coating without inhibitor and hybrid sol-gel coated TAE, TEAE, TME and TME..... 170

Table 4.35 The percentage of an element for the bare mild steel, hybrid sol-gel coated with TSTE extracts fractions on mild steel acquired using EDX analysis 173

LIST OF FIGURES

Page

Figure 2.1 Tamarind (*Tamarindus indicus L*) (Azad, 2018). 8

Figure 2.2 Structural classifications of tannins (Saxena *et al*., 2013). 11

Figure 2.3 Flow diagram representing macroscopic and microscopic forms of corrosion (Zarras and Smith, 2015). 14

Figure 2.4 The mechanism of steel corrosion (Ahmad, 2006). 19

Figure 2.5 The bad and good design of bolted joint (Ahmad, 2006). 23

Figure 2.6 The galvanic system sacrificial anode cathodic protection (Gundogdu and Sahin, 2007). 25

Figure 2.7 The impressed current cathodic protection system (Gundogdu and Sahin, 2007). 26

Figure 2.8 Classification of corrosion inhibitors (Faisal *et al*., 2018). 27

Figure 2.9 Examples of processing routes to obtain sol-gel coatings (Figueira *et al.,* 2016). 33

Figure 2.10 Schematic of rust transformation mechanism of tannin-iron complexes (Zhang *et al.,* 2015). 38

Figure 2.11 A simple Randles'-type equivalent circuit (RC) (Berradja, 2018). 42

Figure 2.12 The Nyquist diagram responding to the simple Randels-type equivalent circuit (Berradja, 2018). 43

Figure 2.13 Bode diagram with respect to the Randels'-type equivalent circuit (Berradja, 2018). 45

Figure 2.14 A Randles'-type equivalent circuit including Warburg impedance component, Z_W. (Helsen and Breme, 1998). 46

Figure 2.15 Electrode kinetics as expressed by the Butler-Volmer equation, plotted Tafel plot showing that the corrosion current density can be obtained from the intercept (Ahmad, 2006). 48

Figure 2.16 Electrochemical current noise fluctuations (Ying and Li, 2012). 52

Figure 3.1	Research flow chat of TSTE extraction, characterization, rust conversion studies, electrochemical studies and surface analysis.	58
Figure 4.1	FTIR spectra of (a) TME, (b) TAE, (c) TWE, and (d) TEAE extract	75
Figure 4.2	Condensed tannin structure.	78
Figure 4.3	Antioxidant profile of TSTE extracts by reducing power assay.	86
Figure 4.4	(a) Thermogravimetric curve (TG) and (b) derivative thermogravimetric curve (DTG) for TME, TAE, TWE and TEAE extracts.	88
Figure 4.5	FTIR spectra of rust standards; (a) lepidocrocite, L (b) goethite, G (c) magnetite, M and (d) salt-spray-generated rust.	90
Figure 4.6	FTIR spectra of rust after 24 h treatment at (a) 1 wt%, (b) 3 wt%, (c) 5 wt%, and (d) 7 wt% of (A) TME and (B) TAE.	93
Figure 4.7	FTIR spectra of rust after 24 h treatment at (a) pH 1, (b) pH 3, (c) pH 5, (d) pH 7, (e) pH 9, and (f) pH 11, with 7 wt% of (A) TME and (B) TAE.	95
Figure 4.8	FTIR spectra of rust upon treatment with 7 wt% of (A) TME and (B) TAE for (a) 1 d, (b) 3 d, (c) 5 d, (d) 7 d, and (e) 14 d of contact time.	97
Figure 4.8(b)	Effect of pH = 3, reaction time = 5 and concentration = 7 on rust transformation.	98
Figure 4.9	Schematic of rust transformation mechanism of tannin-iron complexes.	99
Figure 4.10(a)	XRD patterns of a rust sample. L – lepidocrocite; M – magnetite and G-goethite.	101
Figure 4.10(b)	XRD patterns of the rust sample after treatment with TME rust converter.	101
Figure 4.10(c)	XRD patterns of the rust sample after treatment with TAE rust converter.	102
Figure 4.11	SEM micrographs and EDX spectra of (a) rust powder sample (b) rust powder sample after treatment with TME rust converter (c) rust powder sample after treatment with TAE rust converter at 500× magnification.	104

Figure 4.12 The equivalent circuit of Randles-CPE to fit EIS result of mild steel in 0.5 M HCl solution at different concentrations of TSTE at 303 K. 107

Figure 4.13 The Nyquist impedance curves of mild steel in 0.5 M HCl solution at different concentrations of TME at 303 K. 108

Figure 4.14 The Nyquist impedance curves of mild steel in 0.5 M HCl solution at different concentrations of TAE at 303 K. 109

Figure 4.15 The Nyquist impedance curves of mild steel in 0.5 M HCl solution at different concentrations of TWE at 303 K. 109

Figure 4.16 The Nyquist impedance curves of mild steel in 0.5 M HCl solution at different concentrations of TEAE at 303 K. 110

Figure 4.17 Bode impedance (a) and (b) phase angle plots obtained for the mild steel in 0.5 M HCl solution at different concentrations of TME extract at 303 K. 111

Figure 4.18 Bode impedance (a) and (b) phase angle plots obtained for the mild steel in 0.5 M HCl solution at different concentrations of TAE extract at 303 k. 112

Figure 4.19 Tafel polarization curves of mild steel specimens in 0.5 M HCl solution at different concentrations of TME, at 303 K. 115

Figure 4.20 Tafel polarization curves of mild steel specimens in 0.5 M HCl solution at different concentrations of TAE at 303 K. 116

Figure 4.21 Tafel polarization curves of mild steel specimens in 0.5 M HCl solution at different concentrations of TWE at 303 K. 116

Figure 4.22 Tafel polarization curves of mild steel specimens in 0.5 M HCl solution at different concentrations of TEAE at 303 K. 117

Figure 4.23 The electrochemical current noise plots after 1 h immersion in 0.5 M HC l at 303 K. 124

Figure 4.24 The Arrhenius plots of ln CR versus 1/T at different concentrations of TME. 127

Figure 4.25 The Arrhenius plots of ln CR versus 1/T at different concentrations of TAE. 128

Figure 4.26 The transition state plots of ln CR/T versus 1/T at different concentrations of TME. 129

Figure 4.27 The transition state plots of ln CR/T versus 1/T at different concentrations of TAE. 129

Figure 4.28 Adsorption isotherm plots using Langmuir, equations, upon potentiodynamic polarization measurements at different concentrations (a) TME and (b) TAE at 303 K..... 134

Figure 4.29 Adsorption isotherm plots using Langmuir, equations, upon potentiodynamic polarization measurements at different concentrations (c) TWE and (d) TEAE at 303 K..... 135

Figure 4.30 Schematic corrosion inhibition mechanism of tannin adsorption on the mild steel surface..... 141

Figure 4.31 SEM micrographs of mild steel after 24 h immersion in 0.5 M HCl solution (a) bare mild steel (b) mild steel without inhibitor (c) mild steel with 1000 ppm TME (d) mild steel with 1000 ppm TAE (e) mild steel with 1000 ppm TWE (f) mild steel with 1000 ppm TEAE..... 144

Figure 4.32(a) The equivalent circuit of Randles-CPE to fit EIS result of bare mild steel in 0.5 M HCl at 303 K..... 147

Figure 4.32(b) The equivalent circuit of Randles-CPE to fit EIS result of undoped/ doped TSTE sol-gel in 0.5 M HCl at 303 K..... 148

Figure 4.33 **N**yquist plots of 0.5 M HCl, undoped and TME doped sol-gel coating on mild steel at 303 K. 149

Figure 4.34 Nyquist plots of 0.5 M HCl, undoped and TAE doped sol-gel coating on mild steel at 303 K. 149

Figure 4.35 **N**yquist plots of 0.5 M HCl, undoped and TWE doped sol-gel coating on mild steel at 303 K. 150

Figure 4.36 **N**yquist plots of 0.5 M HCl, undoped and TEAE doped sol-gel coating on mild steel at 303 K. 150

Figure 4.37 Bode impedance (a) and (b) phase angle plots obtained for the mild steel in 0.5 M HCl solution at different concentrations of TME Doped hybrid sol-gel coatings. 151

Figure 4.38 Bode impedance (a) and (b) phase angle plots obtained for the mild steel in 0.5 M HCl solution at different concentrations of TAE Doped hybrid sol-gel coatings. 152

Figure 4.39 Tafel curves for hybrid coatings in 0.5 M HCl solution with various TME content and their comparison with the bare mild steel at 303K. 159

Figure 4.40 Tafel curves for hybrid coatings in 0.5 M HCl solution with various TAE content and their comparison with the bare mild steel at 303K. 159

Figure 4 41 Tafel curves for hybrid coatings in 0.5 M HCl solution with various TWE content and their comparison with the bare mild steel at 303K. 160

Figure 4.42 Tafel curves for hybrid coatings in 0.5 M HCl solution with various TEAE content and their comparison with the bare mild steel at 303K. 160

Figure 4.43 The Arrhenius plots of ln CR versus 1/T of bare mild steel and TME, TAE, TWE, and TEAE doped sol-gel in 0.5 M HCl solution. 166

Figure 4.44 The modified Arrhenius plots of ln CR/T versus 1/T of bare mild steel and TME, TAE, TWE, and TEAE doped sol-gel in 0.5 M HCl solution. 167

Figure 4.45 FT-IR spectra of hybrid sol-gel matrix, hybrid sol-gel coating without inhibitor and hybrid sol-gel coated TAE, TEAE, TME and TME. 169

Figure 4.46 Proposed reaction mechanism of hybrid sol-gel synthesis and its adhesion over mild steel substrate. 171

Figure 4.47 SEM micrographs of mild steel after 24 h immersion in 0.5 M HCl solution (a) bare mild steel (b) blank mild steel without inhibitor (c) hybrid sol-gel coated with 1000 ppm TME (d) hybrid sol-gel coated with 1000 ppm TAE (e) hybrid sol-gel coated with 1000 ppm TWE (f) hybrid sol-gel coated with 1000 ppm TEAE. 174

Figure 4.48 Images of water contact angle of (a) bare mild steel, (b) hybrid sol-gel coated mild steel (without inhibitor) (c) hybrid sol-gel coated with 1000 ppm TAE (d) hybrid sol-gel coated with 1000 ppm TWE (e) hybrid sol-gel coated with 1000 ppm TAE and (f) hybrid sol-gel coated with 1000 ppm TME. 176

LIST OF ABBREVIATIONS

AC	Alternating current
ASTM	American Society for Testing and Materials
CE	Counter electrode
DTG	Derivatized thermogravimetry
DC	Direct current
EDX	Energy dispersive X-ray
EIS	Electrochemical impedance
ENM	Electrochemical noise measurement
FTIR	Fourier transform infrared
GAE	Gallic acid equivalent
GPTMS	3-glycidoxypropyltrimethoxysilane
IE	Inhibition efficiency
NMR	Nuclear magnetic resonance
OCP	Open circuit potential
PD	Potentiodynamic polarization
RE	Reference electrode
SCE	Saturated calomel electrode
SEM	Scanning electron microscope
TEOS	Tetraethyl orthosilicate
TGA	Thermogravimetric analysis
TSTE	Tamarind shell tannin extract
TME	Tannin methanol extract
TAE	Tannin acetone extract
TWE	Tannin water extract
TEAE	Tannin ethyl acetate extract

TPC	Total phenolic content
TFC	Total flavonoid content
TTC	Total tannin content
UV-Vis	Ultraviolet-visible
WE	Working electrode
XRD	X-ray diffraction
ZRA	Zero resistance ammeter

LIST OF SYMBOLS

C_{dl}	Double layer capacitance
CE	Catechin equivalent
cm	Centimeter
CPE	Constant phase element
CPE_{dl}	Double layer constant phase element
CPE_{coat}	Coating constant phase element
CR	Corrosion rate
E_a	Activation energy
E_{corr}	Corrosion potential
F	Faraday constant
g	Gram
i_{corr}	Corrosion current density
IE	Inhibition efficiency
m/v	Weight per volume
mA cm^{-2}	Miliampere per centimeter square
M_{ev}	Equivalent weight
mg	Milligram
min	Minutes
mL	Millilitre
mm y^{-1}	Milimetres per year
mm	Millimetre
mpy	mils of penetration per year
mV s^{-1}	Millivolt per year
mV	Milivolt

R	Universal gas constant
R_{coat}	Coating resistance
R_{ct}	Charge transfer resistance
R_n	Noise resistance
R_p	Polarization resistance
R_s	Solution resistance
T	Absolute temperature
v/v	Volume per volume
wt	Weight
Z	Magnitude of the impedance
Z_{cpe}	Impedance of constant phase element
β_a	Anodic Tafel constant
β_c	Cathodic Tafel constant
ΔG_{ads}	Gibbs free energy of adsorption
ΔH	Enthalpy
ΔS	Entropy
η_a	Anodic overpotential
η_c	Cathodic overpotential
θ	Phase angle
θ_{water}	Water phase angle
λ_{max}	Absorption maximum
ρ	Density
σ_I	Standard deviation of current noise
σ_v	Standard deviation of potential noise
$\Omega\ cm^2$	Ohm's centimeter square
$\boldsymbol{\omega}$	Angular frequency

PENILAIAN EKSTRAK KULIT ASAM JAWA (*TAMARINDUS INDICA L*) SEBAGAI PERENCAT KARAT KELULI LEMBUT DALAM MEDIUM BERASID

ABSTRAK

Tujuan penyelidikan ini adalah untuk mengkaji bagaimana penghambat kakisan yang mesra alam untuk sistem media berasid dapat dikembangkan dan digunakan melalui penilaian ekstrak tanin kulit asam jawa (TSTE) yang diasingkan menggunakan metanol (TME), 70% aseton (TAE), air (TWE), dan etil asetat (TEAE). Berdasarkan hasilnya, analisis fitokimia menunjukkan bahawa TME mengandungi bacaan tertinggi bagi kandungan fenolik keseluruhan (TPC), kandungan flavonoid keseluruhan (TFC), kandungan tanin keseluruhan (TTC), dan aktiviti antioksidan dibandingkan dengan ekstrak TSTE lain. Pada bahagian pertama, potensi (TSTE) dalam transformasi karat dikaji melalui teknik inframerah Fourier-transform (FTIR). Spektrum FTIR juga mendedahkan peratusan transformasi karat (RT%) adalah melebihi 90%. Pada bahagian kedua, ekstrak TSTE dikaji sebagai penghambat kakisan keluli lembut dalam larutan HCl 0.5 M dan hasilnya diperhatikan melalui spektroskopi impedans elektrokimia (EIS), polarisasi potensiodinamik (PD), dan pengukuran kebisingan elektrokimia (ENM). Kajian menunjukkan bahawa peningkatan kepekatan hingga 1000 ppm TSTE meningkatkan kecekapan penghambatan masing-masing adalah IE_{TME} = 87.77%> IE_{TAE} = 86.34%> IE_{TWE} = 82.43%> IE_{TEAE} = 80.90%. Pada bahagian ketiga, kajian ini juga menyelidiki aplikasi pelapisan sol-gel hibrida TSTE yang disediakan menggunakan (GPTMS) 3-glisidoksipropiltrimetoksisilan dan tetraetoksisilan (TEOS). Pengukuran

elektrokimia menunjukkan bahawa TSTE sol-gel hibrida didopkan memberikan kecekapan perencatan yang lebih tinggi berbanding dengan lapisan yang tidak ditutup. Analisis mikroskopi elektron imbasan (SEM) menunjukkan peningkatan morfologi permukaan keluli lembut dengan adanya perencat.

EVALUATION OF TAMARIND (*TAMARINDUS INDICA L*) SHELL TANNIN EXTRACTS AS A CORROSION INHIBITOR OF MILD STEEL IN ACIDIC MEDIUM

ABSTRACT

The aim of this research was to study how eco-friendly corrosion inhibitors for acidic media systems could be advanced and used through evaluation of tamarind shell tannin extracts (TSTE) isolated using methanol (TME), 70% acetone (TAE), water (TWE), and ethyl acetate (TEAE). Established by the result, the phytochemical analysis revealed that TME contained the highest content of Total phenolic content (TPC), Total flavonoid content (TFC), Total tannin content (TTC), and antioxidant activities compared to other TSTE extracts. In the first part, the potential of (TSTE) in rust transformation was studied *via* Fourier-transform infrared technique (FTIR). Also, the FTIR spectra revealed the rust transformation percentage (RT %) was > 90%. And the disappearance of major rust peaks as revealed by X-ray Diffraction analysis. In the second part, TSTE was studied for corrosion inhibition of mild steel in a 0.5 M HCl solution and the results were observed *via* electrochemical impedance spectroscopy (EIS), potentiodynamic polarisation (PD), and electrochemical noise measurement (ENM). It was revealed that increasing the concentration up to 1000 ppm of TSTE increased the inhibition efficiency. IE_{TME} = 87.77 % > IE_{TAE} = 86.34 % > IE_{TWE} = 82.43% > IE_{TEAE} = 80.90%, respectively. In the third part, this study also investigated the applications of TSTE doped hybrid sol-gel coatings prepared using (GPTMS) 3-glycidoxypropyltrimethoxysilane and tetraethoxysilane (TEOS). The electrochemical measurements revealed that TSTE doped hybrid sol-gel

provided higher inhibition efficiency compared to undoped coatings. Scanning electrone microscopy (SEM) analysis showed the improvement of the surface morphology of mild steel in the presence of inhibitors.

CHAPTER 1

INTRODUCTION

1.1 Background of the study

Tamarindus indica or locally known as ‘asam jawa’ in Malaysia and ‘tsamiya’ in Nigeria is a leguminous tree (family Fabaceae) bearing edible fruit that is indigenous to tropical Africa. The fruit is an indehiscent legume, sometimes called a pod, 12 to 15 cm in length, with a hard, brown shell (Doughari, 2006). Previous studies have revealed that the *Tamarindus indica* shell contains fiber, tannin, tartaric acid and calcium (Adur *et al.*, 2019). The tannin compounds can be extracted from *Tamarindus indica* shell to be utilised as corrosion inhibitor of mild steel.

Nowadays, metals and alloys constitute the greatest significant group of engineering tools. Low carbon steel refers to mild steel is among the metals usually used for structural engineering applications. With also slight carbon content to more harden, it is cheap, weldable, which also expands the potential uses. The surroundings, where mild steel is applied, may differ from ambient temperatures to high exposure temperatures of reactive gases, from water to soil, from weak to strong chemicals, as well as nuclear radiation to liquid metals (El-Meligi, 2010). Meanwhile, metallic materials that derive in contact with this environment are subject to corrosion due to their aggressive instability. A promising way for the protection of corrosion is by use of durable material.

Though this frequently is difficult due to cost and economics. Thus, the mild steel protection in these surroundings often comprises the addition of a substance or chemicals which transforms the existing rust or decreasing the corrosion rate, either

by decreasing the aggressiveness of the surroundings or by directly protecting the metal. Substances which counter in this method are identified as corrosion inhibitors. Mostly, inorganic compounds such as molybdate, nitrite, phosphate, and chromate are the excellent standard inhibitors of corrosion, due to successful commercial usage of a long history and their outstanding usefulness above an extensive array of environments (Garcia *et al*., 2011). Despite the effective utilisation of inorganic inhibitors, concerns have recently increased the effects of their toxicity on the environment and human health. The environmental regulations of new generation require toxic chemicals replacement with green inhibitors or green chemicals (Mobin and Rizvi, 2017).

Currently, applications of corrosion inhibitors as rust converters and chemical cleaning agents for removing iron-based deposits are the most popular ways of protecting rust. Recently, tannins have been reported to influence the anticorrosive properties of steel (Barrero *et al*., 2001). Tannins can form chelates with iron and other metallic cations due to the vicinity of hydroxyl groups on the aromatic rings. Tannins also have been referred to as rust converters since their presence converts active rust into non-reactive protecting oxides. Protection properties result from the reactions of polyphenolic parts of the tannin molecule with ferric ions, thereby forming a highly cross-linked network of ferric-tannates (Martinez and Stern, 1999).

In Addition, for proper and efficient operation, most industrial production processes need chemical cleaning, and the most frequently used pickling fluid is water that contains sulphate and chloride ions used to remove depositions, scales, and biological growth from the structural surfaces, which are identified to be aggressive to mild steel (El-Meligi, 2010). The purpose of the addition of inhibitors into the aggressive medium is to slow or delay the interactions among the medium's

corrosive species and the metal. Organic compounds with heterocyclic ring together with a lone pair of electrons acted as active inhibitors of corrosion via adsorption onto the surface of the metal (Quinet *et al*., 2007; Yasakau *et al*., 2008; Zheludkevich *et al*., 2007). Furthermore, heteroatoms containing organic compounds such as nitrogen, oxygen, sulphur and thus containing conjugated π bonds have been extensively studied to reduce the corrosion rate of alloys and their metals (de Souza *et al*., 2014; Hassan *et al*., 2007; Tebbji *et al*., 2005). Mostly organic inhibitors performed through adsorption onto surfaces of the metal on both cathodic and anodic sites, which effect in the protection of both cathodic and anodic reactions (de Souza *et al*., 2014; Kumar *et al*., 2017).

However, hybrid organic-inorganic Sol-gel films are the most encouraging procedures for toxic coatings replacement (Zheludkevich *et al*., 2005). The technology through sol-gel as well offers additional key benefits such as the low impact on environmental, low application cost, and simple procedure that is simply compliant to the industry. Moreover, their adhesion is so effective to metal surfaces through bonding chemically as well as good physical organic topcoats adhesion. Sol-gel metallic protective coatings of this type can only offer passive protection of corrosion. The pores and defects existing in the coatings permit the oxidizing species to enter into the metallic substrate. In order to prevent this constraint, effective inhibitors of corrosion were further applied into the sol-gel medium to promote the metallic anti-corrosion properties (Montemor *et al*., 2009; Wang and Akid, 2008; Montemor and Ferreria, 2008; Voevodin *et al*., 2005). Organic inhibitors of corrosion remain further added to the sol-gel solution. Though several extracted organic inhibitors from plants sources are biodegradable and do not comprise toxic compounds and heavy metals. A successful introduction of a highly efficient green

corrosion inhibitor in acidic media will lead to a flourishing of the acidizing treatment industry and maximize the recovery of the energy resources.

1.2 Problem statement

Unluckily, certain of the very effective corrosion inhibitors previously used for mitigating corrosion risks such as arsenic and chromate are extremely toxic. The increased environmental awareness and the regulations newly developed have enforced limitations on the usage of such inhibitors. Furthermore, safe disposal of corrosion inhibitors after being used is serious and commonly defined as a stage in any treatment chemical programs, which increases a margin to the cost of inhibition program. Many regions and countries are presenting a sequence of adjusting guidelines around the world to provide strategies on the usage and release of the toxic chemicals, particularly salts of heavy metals and inorganic salts. The safety and environmental worries associated with the inhibition procedures have stimulated scientists to discover substitutes for corrosion inhibitors that are eco-friendly, and at the same time can offer acceptable inhibition efficiency, especially in any acidizing treatment process.

Tamarind shell is considered as a waste and disposed of in huge quantities after collecting the pulp in Nigeria. The utilization of this natural biomass could add economic value and improve the livelihood of the people in the region. Tamarind shell extracts contain many organic compounds with a significant number of polyphenols, such as tannin and lignin. These compounds can interact with iron which can result in the inhibition of iron adsorption (Tuntipopipat *et al*., 2009).

Literature review shows that tannin from tamarind shell has not been used in corrosion studies.

The technology through hybrid sol-gel offers additional key benefits such as the low impact on environmental, low application cost, and simple procedure that is simply compliant to the industry. Moreover, their adhesion is so effective to metal surfaces through bonding chemically. The protective coatings of this type can only offer passive protection of corrosion. The pores and defects existing in the coatings permit the oxidizing species to enter into the metallic substrate, leading to pitting corrosion, which is a major drawback. In order to prevent this constraint, effective inhibitors of corrosion were further applied into the sol-gel medium to promote the metallic anti-corrosion properties.

1.3 Research objectives

The purpose of this research was to explore the possibility of using tamarind (*Tamarindus indica L*) shell tannin extract as a green corrosion inhibitor of mild steel in acidic solutions as an alternative to the inorganic corrosion inhibitors that are commonly used in industrial processes. The objectives are as follows:

1) To extract and characterize tamarind shell tannin through complementary analysis.
2) To investigate the potential of tamarind shell tannin extract on rust (iron oxide) transformation via the effect of concentration, pH and reaction time.
3) To analyse the corrosion inhibition efficiency of tamarind shell tannin extract on mild steel substrate through electrochemical measurement and surface analysis.

4) To suggest an appropriate mechanism of corrosion inhibition by employing thermodynamic studies and adsorption isotherm data.
5) To investigate corrosion inhibition performance of tamarind shell tannin extract doped hybrid sol-gel coatings and uncoated substrate via electrochemical and surface analysis.

1.4 Scope of the research

This research comprised the investigation of green plant-based extracted compounds from tamarind shell (*Tamarindus indica L*) to be proposed as a potential corrosion inhibitor of mild steel substrate. The study included effect of concentration, pH and reaction time on rust transformation while the inhibition efficiency was investigated via the effect of inhibitor concentration and effect of temperature. The thermodynamic activities were studied using Arrhenius and transition states equations. Furthermore, the adsorption mechanism was interpreted through Langmuir, Frumkin and Temkin isotherms. In addition, the study also covered the incorporation of tamarind shell tannin into hybrid sol-gel coatings. Lastly, the potential of rust transformation, corrosion inhibition and coating performances were examined using characterization, electrochemical measurement and techniques of surface analysis.

1.5 Limitation of the research

The current research was limited to corrosion inhibition studies using 0.5 M HCl as the medium. Therefore it is suggested to carryout further studies using different HCl concentrations or different medium. In addition, studies should also be carried out using other metal substrates such as copper, aluminium etc. Besides Tamarind shell. other components of Tamarind tree such as leaves and barks which are under utilized should also be tested as corrosion inhibitors. Furthermore, other organic-inorganic precusors apart from GPTMS and TEOS should be used in hybrid sol-gel coatings. Moreover, the disposal of used inhibitor and the leaching of toxic chemicals are other issues that needs to be addressed.

CHAPTER 2

LITERATURE REVIEW

2.1 Tamarind

Tamarind (*Tamarindus indicus L*) *T. indicus* (Figure 2.1) belongs to the family Fabaceae (Leguminosae) from sub-family Caesalpinioideae. It is a semi-evergreen tree, pinnately compound leaves which are largely alternately arranged. It may be extended up to 10-20 m in height. It has pale yellow flowers and is marked with red colour. However, the flowers give a yellowish tint to the tree when it is in full bloom. They have thick fruits; the pods are rough that are usually long about 4-13 cm and are curved. Each pod comprises 1-10 seeds embedded in a pulp that surrounded the seeds which is brown, sticky, fibrous edible and but sour taste. Tamarind is generally established in the subtropics and tropics, not because for its fruits only, however, also as a shade ornamental tree. Tamarind trees are, at times, trimmed into bonsai in Thailand (Mabbery, 2008).

Figure 2.1: Tamarind (*Tamarindus indicus L*) (Azad, 2018).

Tamarind grows wild in tropical Africa's drier parts, where it is native possibly. It has currently extent into other Africa countries, tropical Asia and India, and also West Indies, South America, and major Indian Ocean islands (Diallo *et al.*, 2007). Tamarind seeds comprise 5.5 % fat, 16 % protein, and 63 % starch. It can be consumed as a pulse; however, Tamarind is well known for its pulp pod, which contains about 40 % of the pod. The pulp is rich in vitamin, especially vitamin C and it contains citric acid, malic, tartaric and also sugars, it has a sour-sweet flavour which is used in various drinks, curries, chutneys and sweetmeats. It is an important component in the sauce of Worcestershire. The fruit pulp is known to be the richest natural tartaric acid source, 8-18%. It is the major acidulant, i.e., additive of food used in increasing acidity and tartness in the preparation of India foods (Shankaracharya, 1998).

Tamarind pulp is protein-rich about 8%; it has around 1% crude fat content and approximately 56% carbohydrate content (Amoo *et al*., 2012). Shankaracharya (1998) reported that the Tamarind tree produces fruits 150-500 kg per tree annually, in India, production is around 300,000 metric tons annually. Parvez *et al*. (2003) found that Tamarind root exudates are potent allelochemicals which may explain the weed-free zone frequently observed around Tamarind trees. Sudjaroen *et al*. (2005) reported the quantitative analysis of tamarind pericarp and seeds polyphenolic compounds by analytical HPLC, where the yields were TPC= 6.54 and 2.82 g kg^{-1} seeds and pericarp, correspondingly. In Addition, due to the tannin compound present in tamarind shell, it could serve as a potential corrosion inhibitor.

Tamarind fruit shell is the outer shell of the tamarind pulp and is a by-product of the tamarind pulp industry. It is thus considered as an underutilized or waste material. Currently, it is used mainly as solid fuel and has been used as a biosorbent

for the removal of chromium (Popuri *et al*., 2007). X-ray diffraction analysis of tamarind fruit shell indicates the presence of mostly carbohydrates along with calcium and iron components (Salukha and Kadam, 1995)

Sivasankar *et al*. (2012) reported the application of Tamarind (*Tamarindus indica*) fruit shell (TIFSs) carbon, a calcium-rich promising adsorbent for fluoride removal from groundwater. They were impregnated with ammonium carbonate and then carbonized, leading to ammonium carbonate activated ACA-TIFS carbon. The resulting materials and carbon arising from virgin fruit shells V-TIFS were characterized and assayed as an adsorbent for the removal of fluoride anions from groundwater. The fluoride removal capacity of TIFS carbons was found to be 91% and 83% at a pH of 7.05 for V-TIFS and ACA-TIFS carbons, respectively.

Saha (2010) presented the assessment on the removal of methylene blue dye using tamarind fruit shell as a biosorbent. Various factors affecting adsorption, such as agitation, pH, initial dye concentration, contact time, and temperature, were investigated. The dye adsorption capacity was strongly dependent on solution pH as well as temperature. The Langmuir isotherm model showed a good fit to the equilibrium adsorption data, and the maximum adsorption capacity obtained was 1.72 mg g^{-1} at 303 K.

2.2 Tannins

Tannins are defined generally as astringent, soluble complex phenolic plant origin substances used in proteins precipitation or animal skins tanning. Tannins are also defined chemically as compounds of phenylpropanoid frequently condensed to the variable length of polymers. Compounds of phenolics are defined chemically as

compounds comprising aromatic hydroxylated rings, and the hydroxy group is directly attached to substituted phenyl, phenyl, or other groups of aryl. Phenolic compounds and tannins are secondary plants metabolites that are widely distributed and play a prominent part commonly in plants defence strategies, as well as food quality influence. Based on higher plants' metabolite profile, the relations 'hydrolyzable' and 'condensed' tannins are used to differentiate among the two significant types of tannins vegetable origins, that is gallic acid-derived that are hydrolyzed freely, and flavan-3,4-diol-derived type, that is not hydrolysed readily, respectively. Structurally, tannins are divided into four main groups, such as ellagitannins, gallotannins, condensed tannins, and complex tannins, (Jan and Abbas, 2018) as shown in Figure 2.2.

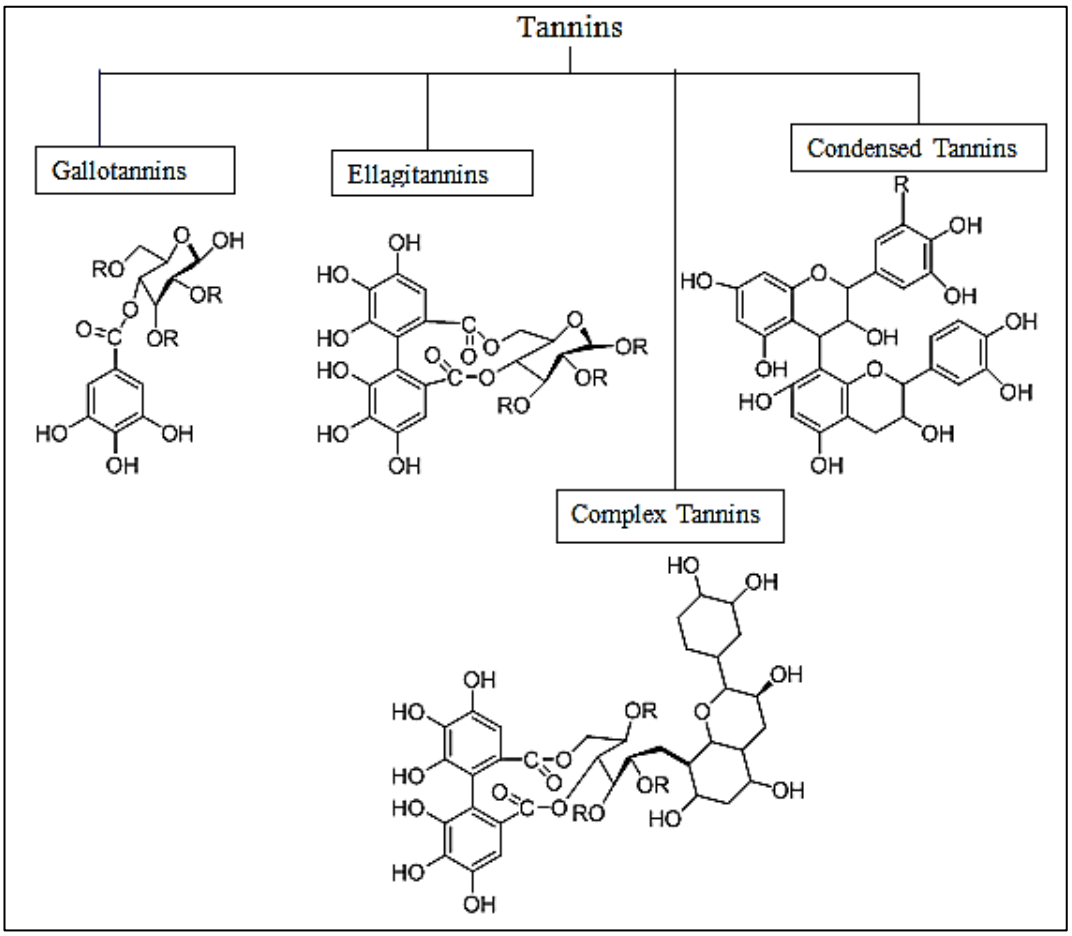

Figure 2.2: Structural classifications of tannins (Saxena *et al*., 2013).

Gallotannins are tannins in which a single unit of galloyl or their derivatives metadepsidic is linked glycosidically to various catechin, triterpenoid or polyol units. Ellagitannins tannins are those type in which two galloyl units at least are coupled C-C to one another. However, they do not comprise a glycosidically catechin linked unit. Complex tannins are tannins in which an ellagitannin or a gallotannin group is bounded glycosidically to catechin unit. Condensed tannins are polymeric and oligomeric proanthocyanidins that are formed by C-4 of one catechin unit linkage with C-8 or C-6 of the next catechin monomer unit (Khanbabaee and Van Ree, 2001).

Tannins are found mostly in fruits such as blueberry, forages, grapes, and legume trees like Sesbania spp, *Tamarindus indica*, and Acacia spp. Moreover, tannins are found in grasses, such as sorghum, and in tea leaves, (Giner-Chavez, 1996). Tannins are essential, which originate from having a significant usage in curing several diseases, such as duodenal tumors, diarrhea, and stomach disorders (De Bruyne *et al*., 1999), and are also used as an antioxidant, antiseptic, anti-inflammatory and pharmaceutical hemostatic (Dolara *et al*., 2005). They are becoming extensive due to their potentials to impede the deterioration of various substrates in a highly corrosive medium (Dargahi *et al*., 2015). The possibility of tannin as an inhibitor of corrosion from different plants such as tannic acid (η_{max} = 86.0) (Qian *et al.,* 2013), mimosa tannin (η_{max} = 87.3) (Martinez and Stern, 2001) and mangrove tannin (η_{max} = 89.9) (Rahim *et al*., 2007) has been investigated.

For more than decades, tannins extracted from renewable resources have been used to protect steam boilers at levels significantly above ASME guidelines. Using tannin-based (green) corrosion inhibitors reduces water and energy consumption,

greenhouse gases emissions, and contaminants in effluent wastewaters while reducing the environmental footprint of industrial processes (Dargahi *et al*., 2015).

Benali *et al.* (2013) reported the inhibitive action of tannin extract of *Chamaerops humilis* plant for the corrosion of mild steel in sulfuric acid. Moreover, the corrosion behaviour of mild steel in 5% EtOH in the presence of tannin extract of *Chamaerops humilis* plant (LF-Ch) and potassium iodide (KI) have been studied using the electrochemical methods. It was found that the inhibition efficiency increased with LF-Ch extract concentration. The addition of potassium iodide to LF-Ch extract in solution increased the inhibition efficiency. A synergistic effect was observed between KI and extract with an optimum concentration of 100 mg/L LF-Ch extract + 0.025% potassium iodide.

Dargahi *et al.* (2015) investigated the surface adsorptive and corrosion protective properties of a commercial tannin-based corrosion inhibitor (TG 3300) for mild steel in an alkaline environment. Quartz crystal microbalance with dissipation monitoring, open circuit potential, and electrochemical impedance spectroscopy (EIS) were used for their study. The results showed the formation of an effective and stable tannin-based protective layer on mild steel within the first 5 min to 15 min of adsorption. The results suggest the formation of a TG 3300 protective layer on mild steel, where the highest value of inhibition efficiency was 85% under the applied experimental conditions.

2.3 Brief overview of corrosion

Corrosion is generally described as the destruction of metallic material by contact with its surroundings (Bardal, 2007). Typically, when describing corrosion,

some talk about metals; however, non-metals such as rubber, plastics, ceramics, as well can experience deterioration or destruction once exposed to different aggressive environments. Corrosion can be visible or invisible, as shown in Figure 2.3. Visible corrosion is the one that can be prevented and controlled; on the other hand, invisible ones cause severe damage and catastrophic failure.

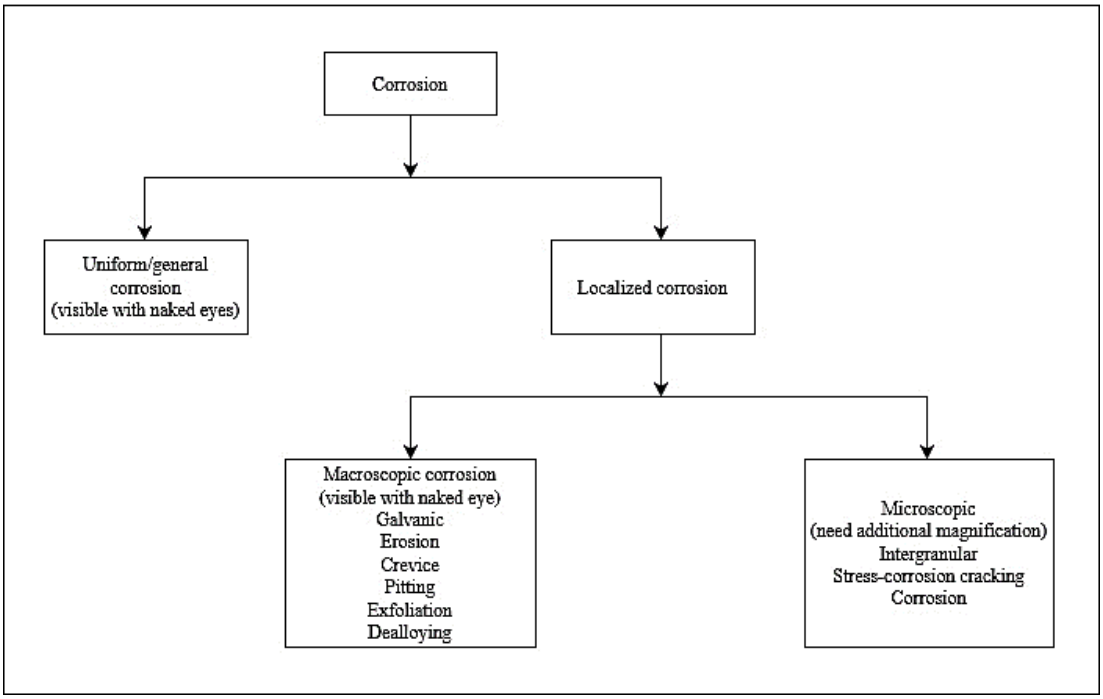

Figure 2.3: Flow diagram representing macroscopic and microscopic forms of corrosion (Zarras and Smith, 2015).

The metallic corrosion is an oxidation-reduction reaction, whereby the uncharged metallic atom loses its electrons and becomes a charged metallic ion:

$$M \leftrightarrow M^{+} + \text{electron} \qquad (2.1)$$

Initially, the metal ion in an ionizing solvent goes into solution and then experiences a secondary reaction, relating with additional ions existing in the surroundings towards forming an insoluble molecular species such for example

aluminium oxide or rust. In oxidation at elevation temperature, the metallic ion becomes lattice part of the oxide formations. Thus, corrosion is classified by three major forms (Bardal, 2007):

(a) Wet corrosion

(b) Corrosion in other fluids

(c) Dry corrosion

Wet corrosion discusses the metallic corrosion occurring in an aqueous/wet environment which is virtually an electrochemical process, and it occurs on a metal surface when an electrochemical reactions proceeds. When an aggressive aqueous/wet environment is exposed to a metal, the metal's nature is changed fundamentally and dissolved becoming into a non-metallic form of species and or form products of corrosion. The system drive energy is depressed as the steel metal changes to a further form of stability; thus, the non-metallic consequences of corrosion. Therefore, the process of electrochemical reactions can occur nonuniformly or uniformly through the surface of the metal, known as the electrode and the conducting ionic liquid is termed the electrolyte. A rusting of a mild steel substrate is an example of this process; the metal iron is transformed into a non-metallic state known as "rust" (Marek and Natalie, 1998).

Corrosion in other fluids discusses the alloys/metals corrosion in non-aqueous environments, for example, molten salts, i.e. fused salts (Kroger, 1998). However, deterioration can also happen in fluid metals, fused salts such as oxides, hydroxides, sulfates, carbonates, nitrates, and halides can originate intense deterioration on alloys and metals through a number of mechanisms: (1) pitting as a result of electrochemical deterioration, (2) mass conveyance because of the thermal inclines,

(3) reactions of fused salt components with alloys and metals, and or (4) reactions of fused salts with impurities present. However, in addition to fused salts, metals and alloys exposure to fluid-metal surroundings can originate corrosion severely. Industrial applications used liquid metals as reducing agents at high temperature or as heat transfer coolants owing to their outstanding properties. Corrosion in liquid-metals can cause impurity, dissolution, alloying, compound reduction and interstitial reactions (Tortorelli, 1998).

Dry corrosion discusses the deterioration of alloys and metals which are affected as a result of exposure to aggressive gases or air. However, for a few metals, contacting to gases does not promote corrosion, although, most of the metals, a high gaseous temperature exposure results in corrosion failure and increases the rate of corrosion (Bradford, 1998). There are various types of corrosion which originate from aqueous or wet surroundings and further identified through deterioration appearance on the metals and alloys. These include general or uniform corrosion, pitting corrosion, crevice corrosion, Galvanic corrosion, erosion-corrosion, intergranular corrosion, dealloying corrosion, environmentally cracking assisted corrosion, i.e. cracking, stress-corrosion, hydrogen damage and corrosion fatigue (Zarras and Smith, 2015).

2.4 Corrosion of steel

A surface of metal exposed to an aqueous conducting electrolyte commonly becomes the location for redox chemical reactions to takes place. There is an anodic reaction or oxidation that releases electrons as, in Equation 2.2 (Ahmad, 2006):

$$Fe \rightarrow Fe^{2+} + 2e^{-} \quad (2.2)$$

A cathodic reaction accepts the electrons released by the oxidation reaction such as the following equations:

$$O_2 + 2H_2O + 4e^- \rightarrow 4OH^- \quad (2.3)$$

$$O_2 + 4H^+ + 4e^- \rightarrow 2H_2O \quad (2.4)$$

$$2H^+ + 2e^- \rightarrow H_2 \quad (2.5)$$

The reaction at the cathodic site represented by Equation (2.3) is typically the most significant to natural environmental corrosion since such corrosion takes place at values nearly to neutral pH. Nonetheless, Equations (2.4) and (2.5) must also be considered for the acidic environments encountered in industrial processes or for the confined volumes, where the pH can reach acidic values because of hydrolysis reactions such as Equation 2.6

$$Fe^{2+} + 2H_2O \rightarrow Fe\,(OH)_2 + 2H^+ \quad (2.6)$$

which produces H^+ ions, the concentration of which can become large because the H^+ ions cannot move out readily from the confined volume (Kruger and Begum, 2016).

Nevertheless, owing to the instability of iron (II), it does oxidize further to iron (III) ions, which is more stable. as shown in Equations 2.7:

$$4Fe^{2+} + 8H^+ + 2O_2 \rightarrow 4Fe^{3+} + 4H_2O \quad (2.7)$$

The iron (III) ions further react with ions of hydroxide to yield hydrated reddish-brown colour substance called rust [iron (III) oxides] as shown in Equation 2.8 (Kruger, 2001).

$$Fe^{3+} + 3OH^{-} \rightarrow Fe(OH)_3 \quad (2.8)$$

In the presence of hydrochloric acid (HCl), unstable ferrous chloride, and hydrogen gas will be produced as in Equation 2.9 (Kruger, 2001).

$$Fe + 2HCl \rightarrow FeCl_2 + H_2 \quad (2.9)$$

However, $FeCl_2$ will oxidize further yielding ferric hydroxide as in Equation 2.10 (Tamura, 2008):

$$FeCl_2 + \tfrac{1}{4} O_2 + 2\tfrac{1}{2} H_2O \rightarrow Fe(OH)_3 + 2HCl \quad (2.10)$$

In addition, $Fe(OH)_3$ can oxidize further to dehydrated oxyhydroxide as in Equation 2.11 (Kruger, 2001):

$$Fe(OH)_3 \rightarrow FeOOH + H_2O \quad (2.11)$$

At last, $Fe(OH)_3$ will undergo further oxidation to produce goethite (α-FeOOH), β-FeOOH (akaganite), γ- FeOOH (lepidocrocite), and Fe_3O_4 (magnetite), respectively.

Since these anodic and cathodic reactions occur simultaneously on a metal surface, they create an electrochemical cell of the type as shown in Figure 2.4. The

locations where both reactions (cathodic and anodic) occur, i.e. the cathode and the anode of the corrosion cell, are determined by various aspects;

(a) They need to be fixed in a location that can be widely separated or adjacent, such that, two metals contact, one can be the cathode and the additional, the anode, which results in galvanic corrosion of the more anodic site metal.

(b) Variation of oxygen concentration over the surface in the surroundings can cause the formation of the anode at the lower oxygen content sites that are exposed to the surroundings.

The dissolution of the metal in the electrolyte occurring at the anodic sites form metallic ions and subsequently into oxides as a result of the conversion of these ions into rust. This destructive process is known as 'corrosion'. The electron flow between the oxidizing anode and the reducing cathode determines the corrosion current generated, which is caused by the rate of electron production by the reaction at the anodic site and their consumption by the cathodic site of the reaction (Kruger and Begum, 2016).

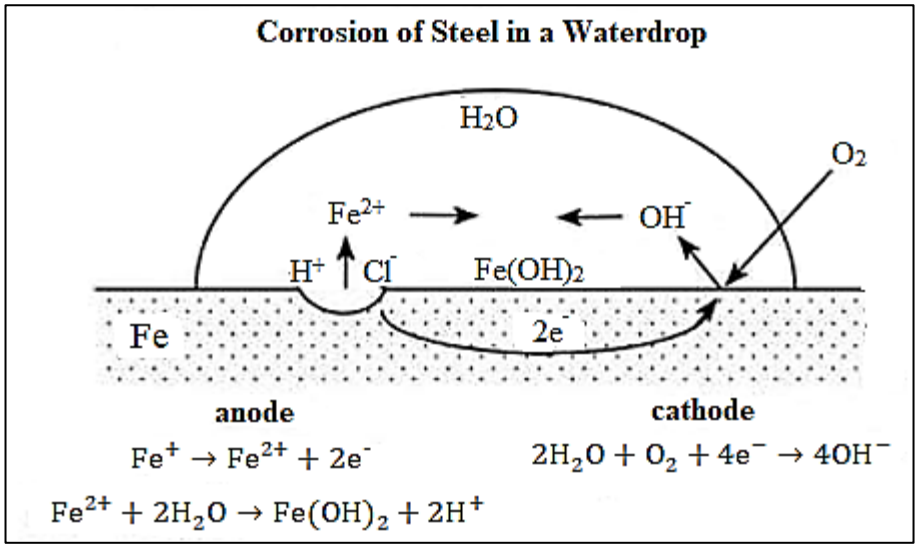

Figure 2.4: The mechanism of steel corrosion (Ahmad, 2006).

2.5 Consequences of corrosion

The plant failure by corrosion can be catastrophic or gradual. Plants' progressive failure has safety implications. Gradual or catastrophic plant failure through corrosion can result in the product loss from a failed reactor vessel at high velocity, and also from a steam line to high-energy steam, inflammable or toxic materials from storage vessels. Instances from plants of this nature around the world have led to the injury of plant operatives, in some cases causing death and also affect the nearby householders. The majority of severe cases occur in the chemical process industry; however, it has been known to cause mechanical failure (Schofield, 2002).

Furthermore, the metal lost from the inside of reaction vessels, pipework, pumps, typically leads to contamination of the product. Thus, the effects of this directly influence the product. White plastics get discoloured even in the presence of ppb levels of iron. The beer taste is affected by iron concentration and other metals. However, products traded to compositional supplies such as acid grade-reagent can be damaged by pick-up metal. Medicinal products for human use are usually powders, or white tablets can simply get discoloured by slight corrosion products' contamination (Schofield, 2002).

2.6 Economic implications of corrosion

The major financial implications of plant corrosion are the initial construction cost, the cost of replacement and maintenance, and the production loss as a result of unexpected shutdowns. The selection of material influences the initial plant cost of construction, and a material of choice which is more resistant to corrosion than is essential for safer plant operation above its design existence is very expensive. This

cost comprises the initial amount of money since the inappropriate selection of materials could lead to unprofitable plant operations (Schofield, 2002). Furthermore, the United States' direct corrosion costs ought to be estimated at U.S. dollars ~$300 billion annually, figuring for gross domestic product, approximately 3.4% (GDP). Industrialized world concluding to the costs of corrosion, which account for roughly $2.5 trillion U.S. dollars, thus, signifies the world's GDP of over 3.4% (Koch, 2016). Also, a comprehensive investigation was carried out by NACE to establish corrosion costs, which revealed that the annual cost of corrosion in Malaysia is about RM6.7 billion which account for RM207.4 billion of GDP (Saupi *et al*., 2015). Hence, to cut the corrosion cost upsetting several national economies, corrosion effective approaches must be engaged. The present corrosion-preventing skills comprise (1) proper industrial design; (2) suitable materials selection (metals, alloys, plastics,); (3) cathodic protection (4), inhibitors, coatings and surface treatment.

2.7 Corrosion control

2.7.1 Material selection

Selection of a material resistant to corrosion for the environment is essential to a well-intentioned design. Design and material are complementary to one another, and either of the two can be overlooked. The material selection procedure for the replacement of the original plant is vital to the economy and safe to the plant operation. Selection of material is also thoughtful to engineering design. By employing a proper design, corrosion may be reduced. A key factor for corrosion control strategy in a given environment is the selection of appropriate materials. The selected material has to meet the standards for the strength of mechanical operations,

corrosion and erosion resistance for conditions under specific service. For example, highly corrosion resistive alloys are employed for piping systems and valves in destructive environments, such as chemical processing plants and refineries. The alloy or metal must have known compatibility with the detrimental surroundings. For example, stainless steel (SS) 316 with 2% Mo for seawater operation is a better material than (SS) 304 without molybdenum. Bronze, copper and brass, and based alloys for saltwater transportation are highly desirable, though, for an environment containing ammonia. They are commonly susceptible to be employed in agriculture. A good design for corrosion prevention against aggressive environments is a vital parameter (Ahmad, 2006).

2.7.2 Proper design

However, a subsequent corrosion action has significant implications on the design of a plant, Figure 2.5. Proper design reduces the risks of corrosion where bad design helps or intensifies corrosion. As stated, prevention of corrosion must start at the writing board, at the stage of design. An improper design is an added cost than a proper design at a writing board; in reality, an incorrect design is continuously much costly than an appropriate design. The aspects of the design include technical design that openly stands on the proper product attributes of technical functioning that define how it is made and how it's working. The service life of components has a critical role to play in design configuration.

The most important point for designers is to understand and to have an awareness of the problems of corrosion. Corrosion is one of the numerous factors which concerns the designer, though; important attention in designing perspective is

to consider corrosion before detected by a condition. In several occasions, incorporation of corrosion prevention in the design of tools is merely after its early failure. Further, more attention has to be made on a specific environment in the selection of corrosion-resistant materials, and minimal attention is given to design, which leads to failure of equipment. For example, even a copper-nickel material, such as 90-10 may prematurely fail as a material condenser tube if the velocity flow of seawater has not taken into consideration in the tube design for a smooth flow (Ahmad, 2006).

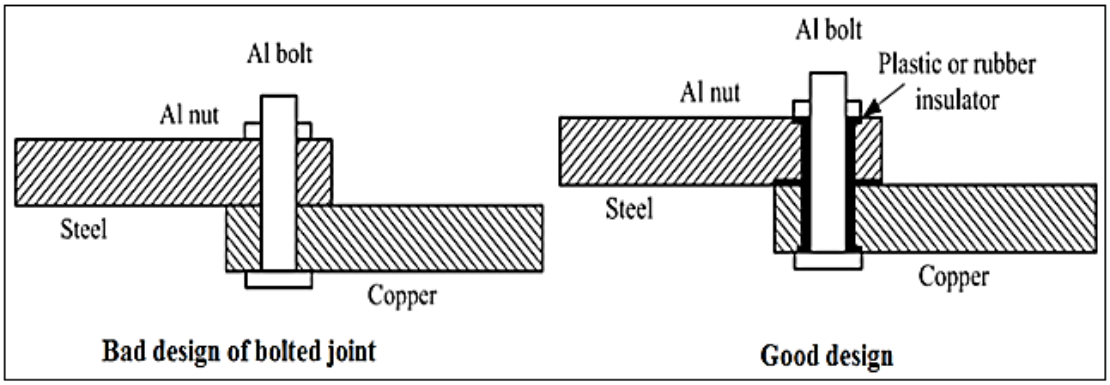

Figure 2.5: The bad and good design of bolted joint (Ahmad, 2006).

Furthermore, electrical protection can also minimize corrosion (cathodic or anodic protection). Cathodic ways of protection is a process of reducing deterioration by reducing the potential change among cathode and anode. This is attained by protecting a structure by applying a source of current, for instance, a pipeline from certain external basis. When applied current is enough, the entire construction to be protected will be at single potential; accordingly, the sites of cathode and anode could not exist. Prevention through cathodic means is usually used on various structural types, such as ship hulls, storage underground tanks and pipelines. The

main forms of protection by cathodic methods are (i) Galvanic method (sacrificial anode system) and (ii) impressed current system (Schofield, 2002).

2.7.3 Galvanic method

Galvanic method (sacrificial anode system by cathodic prevention), a Galvanic cathodic method of protection, makes the use of different metals of destructive potentials (Figure 2.6). Without prevention by the cathodic system, a more negative potential exists in one area of the structure than the other side of the structure, and results in corrosion. Though a less inert object that exists, by the potential of more negative, such as a zinc or magnesium is positioned as anode next to the protected structure, such as an underground tank or pipeline, while insulated wire serving as a metallic connector is fixed between the structure and the object. The object becomes the anode and the the entire structure becomes the cathode. So, the novel object sacrificially corrodes to protect the structure; protection by cathode system is named as a sacrificial anode cathodic system of protection since sacrificially, the anode oxidizes to shield the structure. However, Galvanic anod systems are typically prepared by either zinc or magnesium as these metals are related to steel buildings possessing higher potential (Liao, 2014).